Evidence of sub-clinical prion disease in aged mice following exposure to bovine spongiform encephalopathy

Evidence of sub-clinical prion disease in aged mice following exposure to bovine spongiform encephalopathy

Running title: Aging dramatically impairs BSE transmission

Contents category: Other (TSE) agents

Karen L. Brown[1] and Neil A. Mabbott[1]*

[1]The Roslin Institute and Royal (Dick) School of Veterinary Sciences, University of Edinburgh, Edinburgh, UK.

*, Corresponding author:

Mailing address: The Roslin Institute and Royal (Dick) School of Veterinary Sciences, University of Edinburgh, Roslin, Midlothian EH25 9PS, UK

Tel: +44 (0)131 651 9000; Fax: +44 (0)131 651 9000

E-mail: neil.mabbott@roslin.ed.ac.uk

Word count :

Summary: 241

Main body: 5283

No. Tables: 1

No. Figures: 6

Supplementary Figures: 1

Summary

The occurrence of variant Creutzfeldt-Jacob disease (vCJD) in humans was almost certainly the result of consumption of food contaminated with bovine spongiform encephalopathy (BSE) prions. Despite probable widespread exposure of the UK population to BSE-contaminated food in the 1980s, vCJD has predominantly been identified in young individuals, and there have been fewer cases of clinical disease than anticipated. The reasons for this are uncertain. Following peripheral exposure many prions replicate within the lymphoid tissues before infecting the CNS. We have shown that the effects of host age on the microarchitecture of the spleen significantly impair susceptibility to mouse-adapted prions after peripheral exposure. The transmission of prions between different mammalian species is considered to be limited by the "species barrier," which is dependent on several factors including an intact immune system. Thus, cross-species prion transmission may be much less efficient in aged individuals. To test this hypothesis, we compared prion pathogenesis in groups of young (six to eight weeks old) and aged (600 d old) mice injected with primary BSE. We show that prion pathogenesis was dramatically impaired in aged mice when compared to young animals. Whereas most young mice succumbed to clinical prion disease, all aged mice failed to develop clinical disease during their lifespans. However, the demonstration that prion accumulation was detected in the lymphoid tissues of some aged mice after injection with primary BSE, in the absence of clinical signs of prion disease, has important implications for human health.

INTRODUCTION

Transmissible spongiform encephalopathies (TSEs) or prion diseases are sub-acute neurodegenerative diseases which affect humans and animals. These diseases are defined by a number of characteristic pathological changes in the central nervous system (CNS) including vacuolation of the neuropil, gliosis and aggregations of PrP^{Sc} an abnormally folded isoform of the cellular prion protein (PrP^{c}). The precise nature of the infectious prion is uncertain, but PrP^{Sc} is considered to constitute the major, if not sole, component (Bolton *et al*., 1982, Legname *et al*., 2004).

In 1996 a "new variant" of CJD (vCJD) was described in 10 individuals with a clinical and pathological phenotype distinct from that of sporadic (s)CJD (Will *et al*., 1996). Transmissions to mice have produced compelling evidence to show that brain material from vCJD affected individuals produces a signature undistinguishable from that of BSE (Bruce *et al*., 1997). The components of this signature include; distinct incubation periods in specific mouse strains; distinct neuropathological characteristics in the brains of recipient mice; and distinct PrP^{Sc} glycoforms (Somerville *et al*., 2005). One of the most striking features of vCJD is the young age of the affected individuals (median age at onset of disease ~26 years old) (Boelle *et al*., 2004, Ghani *et al*., 2000) (Fig. S1). Of the 177 recorded definite and probably vCJD cases which had been reported in the UK at the time of writing (August 2013), the majority had occurred in young patients, with only 5 cases (2.8%) observed in the eldery (≥60 years old). This contrasts starkly with those affected with sCJD which typically affects individuals >60 years old. The reasons behind this apparent age-related susceptibility are

not fully understood. A causal link between dietary preference (the consumption of foodstuffs considered to be at high risk of BSE contamination) and disease incidence in the young has not been substantiated (Boelle *et al*., 2004), suggesting that other factors may significantly influence susceptibility.

Although the major pathology associated with prion infection appears to be restricted to the CNS, the peripheral immune system plays an essential role in the pathogenesis of many natural and experimental prion diseases (Mabbott, 2012). Studies with mouse-passaged prions show that following peripheral exposure, early prion accumulation and replication occurs upon follicular dendritic cells (FDC) within the secondary lymphoid tissues prior to the spread of infection to the CNS (termed *neuroinvasion*) (Brown *et al*., 1999, McCulloch *et al*., 2011). Prion replication upon FDC is a critical stage in the neuroinvasion process as disease susceptibility is impaired in their absence (Mabbott *et al*., 2000, Mabbott *et al*., 2003, Montrasio *et al*., 2000). While prion replication in Peyer's patches of the intestine and spleen appears to be dependent upon PrP^{C}-expressing FDC, data from an elegant study has revealed that some prion strains can also accumulate in association with high endothelial venules in lymph nodes (O'Connor *et al*., 2012). Following peripheral exposure to many natural prion diseases, including natural scrapie in sheep (Andreoletti *et al*., 2000), chronic wasting disease (CWD) in cervids (Sigurdson *et al*., 1999), and vCJD in humans (Hilton *et al*., 1998), early agent accumulation also appears to occur first upon FDC within the secondary lymphoid tissues prior to the spread of infection to the CNS. In mammals host age has a significant influence on immune function. In the spleens of aged mice (≥600 d old) FDC status is adversely affected and the

marginal zone (MZ) is disrupted (Aydar *et al*., 2002, Aydar *et al*., 2003, Birjandi *et al*., 2011, Brown *et al*., 2012, Brown *et al*., 2009). Our data show that the effects of aging on the splenic microarchitecture impede the delivery of prion-containing immune complexes from the MZ to FDC, and as a consequence, reduce disease susceptibility to mouse adapted prions (Brown *et al*., 2012, Brown *et al*., 2009).

The transmission of prions strains within the same host species usually occurs efficiently and with highly reproducible disease characteristics (similar incubation periods, neuropathology etc.). However, prion transmission between different species on the first passage are typically characterised by low efficacy and prolonged disease incubation periods: termed the “species barrier” effect. Several factors are known to have an important influence on the species barrier. Data suggest that the species barrier is due to incompatibility between the PrP of the infectious prion and the recipient (host) species, with differences in the PrP species or polymorphisms and mutations in the *PRNP* genotype (which encodes PrP^{C}) having significant influence (Barron et al., 2001, Bishop et al., 2006, Houston et al., 2003, Prusiner et al., 1990). However, the precise molecular mechanism responsible for these effects is uncertain. Studies using immunodeficient mice have shown that a functional immune system is also essential for the efficient cross-species transmission of BSE prions (Brown *et al*., 1997). Severely combined immunodeficient mice (SCID) mice which lack functional, mature FDC in their lymphoid tissues show dramatically reduced susceptibility to prion infection following injection with primary BSE prions. This suggests that the effects of aging on FDC status and the splenic MZ may likewise impede the cross-species transmission of BSE. To test this hypothesis,

we compared primary prion pathogenesis in young and aged mice injected with primary BSE. Our data show that aged mice did not develop clinical disease after BSE exposure. However, some mice had evidence of prion accumulation in their spleens. These data suggest that while aged individuals may be less susceptible to clinical prion disease after BSE exposure, they may accumulate significant levels of prions within their lymphoid tissues and pose a potential risk for the horizontal spread of disease.

RESULTS

Effect of host age on susceptibility to BSE infection

The transmission of BSE to specific inbred strains of mice produces distinctive neuropathological characteristics and reproducible incubation periods (Bruce *et al*., 1997). Here, following primary BSE injection into groups of young (six – eight wk old) RIII mice and young C57BL mice clinical disease was confirmed in the majority of the recipients with incubation periods consistent with previously published data (RIII, 361 ± 8 d; C57BL, 505 ± 27 d; Table 1) (Bruce *et al*., 1997). Histopathological analysis of the brains from the clinically-affected young mice revealed that the severity and distribution of the vacuolar (spongiform) pathology was typical of that associated with BSE transmission to mice (Fig. 1a & 1b) (Bruce *et al*., 1997). The absence of disease in a small number of the young mice (Table 1) was not unexpected since cross species transmission is often less efficient. Of the 17 aged RIII mice that were injected with BSE prions (aged RIII mice were 600 d old at the time of BSE injection), 7 survived until after the first clinically-positive case in the corresponding young mice (aged RIII mice were 928-1041 d old at time of cull; Table 1). However, there was no evidence of clinical disease or positive vacuolar pathology in any of the brains from the BSE-injected aged RIII mice (Fig. 1a & 1c; Table 1). Unfortunately, the disease incubation period after primary BSE injection in C57BL mice (~500 d) exceeded the lifespan of the aged mice in this study (aged C57BL mice were 600 d old at time of BSE injection and survived to ~900 d old). However, histopathological analysis of all the brains from the BSE-injected aged C57BL mice, including 9 animals that survived to over two thirds of the incubation period in the

corresponding young mice, found no evidence of vacuolar pathology (Fig. 1b & 1d; Table 1).

Effect of host age on PrP^{Sc} accumulation in the brain

In addition to vacuolar changes, CNS prion infection is accompanied with astrogliosis, increased microglial activity and abnormal accumulations of disease-specific PrP. As anticipated, all the brains from the BSE-injected, clinically-affected young RIII mice and young C57BL mice with positive vacuolar pathology in their brains demonstrated high levels of astrogliosis and microgliosis consistent with the terminal stage of prion disease (Fig. 2). However, none of the histopathological characteristics of CNS prion disease were detected in any of the brains from the BSE-injected aged RIII mice and C57BL mice (Fig. 2). Together, these data show that BSE disease-susceptibility is dramatically reduced in aged mice.

In this study, two distinct terms (PrP^{Sc} and PrP^{d}) describe the disease-specific, abnormal accumulations of PrP that are characteristically found only in prion-affected tissues. Prion disease-specific PrP accumulations are relatively resistant to proteinase K (PK) digestion, whereas cellular PrP^{C} is destroyed. Thus prion-specific PK-resistant PrP (referred to as PrP^{Sc}) can often be used as a biochemical marker for the presence of prions (Bolton et al., 1982). On histological sections where PK-treatment is not used since it destroys the tissue microarchitecture, we refer to these abnormal disease-specific PrP accumulations as PrP^{d}. However, to confirm the presence of prion-specific PK-resistant PrP^{Sc}, adjacent brain sections were applied to nitrocellulose membrane,

PK-treated and analysed by paraffin-embedded tissue (PET) immunoblot (Schulz-Schaeffer et al., 2000).

Our previous studies of the transmission of mouse-passaged prions to aged mice revealed the presence of prion-specific PrP^{Sc} deposition in the majority of the brains from aged mice after peripheral (intraperitoneal and oral) exposure, despite the absence of clinical signs of disease or vacuolar pathology (Brown *et al*., 2009). We therefore determined whether PrP^{Sc} was present in the brains of the clinically-negative, BSE-injected aged mice. Large accumulations of PrP^{d} were detected by immunohistochemistry (IHC) in the brains of all the clinically affected, BSE-infected, young mice (Fig. 2; Table 1). PET immunoblot analysis of adjacent sections confirmed that the PrP^{d} detected by IHC was PK-resistant, prion-specific PrP^{Sc} (Fig. 2). In contrast, PrP^{Sc} was only detected in a small foci in the brain of one of the BSE-injected aged RIII mice (the vestibular nucleus), and was undetectable in the all the brains from the aged C57BL mice (Fig. 2 & 3a; Table 1).

Effect of host age on the accumulation of PrP^{d} in spleen

The accumulation of high levels of PrP^{Sc} upon FDC in lymphoid tissues is a characteristic feature of many experimental and natural prion infections, and studies in mice show this is a crucial for efficient neuroinvasion. Furthermore, SCID mice that lack mature FDC are also refractory to prion infection after exposure to BSE prions (Brown *et al*., 1997). Here, high levels of PrP^{d} consistent with association upon FDC were detected in almost all the spleens from the prion-infected young RIII mice and C57BL mice (Figure 3, Table 1). In aged

mice, despite the absence of clinical and histopathological signs of disease in the CNS, heavy PrP^{d} accumulations were also detected upon the few intact FDC remaining in the spleens of most of the BSE-challenged RIII mice (9/16) and 2/9 of the C57BL mice (Fig. 3, Table 1).

FDC status is adversely affected in the spleens of aged RIII mice

We have previously shown that the status of FDC and their ability to trap and retain immune complexes are compromised in the spleens of aged C57BL mice (Brown *et al*., 2012, Brown *et al*., 2009). We therefore determined whether aging also adversely affected FDC status in RIII mice. FDC in the spleens of young mice express high levels of complement receptor (CR) 1 and CR2, cellular PrP^{C} and trap and retain large amounts of complement component C4 on their surfaces (McCulloch *et al*., 2013, Taylor *et al*., 2002, Zabel *et al*., 2007) (Fig. 4). The expression of CR2/CR1 by FDC in the spleens of aged mice was similar to that observed in young mice (Fig. 4). However, the majority of FDC networks in the spleens of the aged RIII mice showed reduced expression of PrP^{C} and impaired retention complement component C4 (Fig. 4a), as observed in the spleens of aged C57BL mice (Fig. 4c) (Brown *et al*., 2012, Brown *et al*., 2009). Morphometric analyses confirmed that in the spleens of the aged RIII mice (Fig. 4b) and C57BL mice (Fig. 4d) the number and size of the PrP^{C}-expressing FDC networks, and the level of trapped C4 on their surfaces, were significantly reduced. The expression of PrP^{C} by FDC, and their ability to trap and retain complement-containing immune complexes, are each important for the efficient retention and replication of prions upon their surfaces (Klein *et al*., 2001, Mabbott *et al*., 2001, McCulloch *et al*., 2011, Michel *et al*., 2012, Zabel *et al*., 2007). Our

data show that these characteristics are dramatically affected in the spleens of aged RIII mice (Fig. 4a & 4b) and aged C57BL mice (Fig. 4c & 4d).

Aging adversely affects the distribution of MZ macrophages in the spleens of aged C57BL mice, but not aged RIII mice

The splenic MZ surrounds the white pulp and comprises a distinct channel of mucosal vascular adressin cell-adhesion molecule 1 (MADCAM1)-expressing sinus lining cells through which blood percolates on its way to the red pulp. Specific populations of macrophages and B cells are firmly attached to this network, enabling the continuous surveillance and clearance pathogens, toxins and apoptotic cells from the blood-stream (Mebius & Kraal, 2005). MZ B cells also capture blood-borne immune complexes and rapidly shuttle them to FDC (Cinamon *et al*., 2008). We and others have previously reported that the MZ microarchitecture is disturbed in the spleens of aged C57BL mice, impeding the delivery of immune-complexes and prions to FDC (Birjandi *et al*., 2011, Brown *et al*., 2012). We therefore determined whether similar disturbances to the MZ microarchitecture occurred in the spleens of aged RIII mice. First, we graded the disruption to the network of MADCAM1-expressing sinus lining cells, and detected a significant disruption to this network in spleens from aged RIII and C57BL mice (Fig. 5a & 5b). In young mice, marginal metallophilic (MM) macrophages ($CD169^+$ cells) typically form a continuous thin rim at the inner border of the MZ, but in aged mice this area was likewise thickened, distorted and broken (Fig. 5a). Morphometric analysis confirmed that the MM macrophage layer was also significantly disrupted (Fig. 5c) and significantly thicker (Fig. 5d) in the spleens of aged RIII and C57BL mice, when compared to young mice.

The MZ also contains an outer ring of MZ macrophages expressing the C-type lectin SIGNR1. The distribution of SIGNR1$^+$ MZ macrophages was also significantly reduced in the spleens of aged C57BL mice when compared to young mice (Fig. 6; $P < 0.0003$, Mann-Whitney *U*-test). However, the distribution of the SIGNR1$^+$ MZ macrophages in the spleens of aged RIII mice was similar to that observed in young RIII mice (Fig. 6; $P = 0.16$, Mann-Whitney *U*-test). Together, these data reveal that although the distribution of the MADCAM1$^+$ sinus lining cells and CD169$^+$ MM macrophages was significantly disturbed in the MZ of aged RIII mice (as observed in aged C57BL mice), the distribution of SIGNR1$^+$ MZ macrophages was not adversely affected in the spleens of aged RIII mice.

Discussion

Here we show that the susceptibility of aged mice to prion disease after exposure to primary BSE is dramatically reduced. Furthermore, there were no histopathological signs of prion disease in any of the brains from the BSE-injected aged mice. In addition, PrP^{Sc} was undetectable in all the brains from the BSE-injected aged C57BL mice and only detected in a small foci (the vestibular nucleus) of the brain of one of the aged RIII mice. An intact immune system is important for cross-species transmission of BSE prions (Brown *et al*., 1997). Here, the effects of aging on prion susceptibility after BSE-exposure coincided with disturbances to FDC and the microarchitecture of the MZ in the spleen. However, despite the absence of clinical and histopathological signs of prion disease in the CNS, heavy PrP^{d} accumulations were detected upon the remaining intact FDC in the spleens of many of the BSE challenged aged RIII mice and some of the aged C57BL mice. The detection of PrP^{d} in spleens of BSE-injected aged mice in the absence of neuropathological signs and clinical disease has important implications for human health and the potential for the horizontal spread of vCJD, for example by accidental iatrogenic transmission.

Following the emergence of BSE in the 1980s it was estimated that over half a million infected cattle may have entered the UK food chain (Valleron *et al*., 2001, Wilesmith, 1993). Despite the probable widespread exposure of the UK population to the BSE agent via contaminated foodstuffs (Valleron *et al*., 2001) the number of confirmed clinical cases of vCJD remains relatively low (Bishop *et al*., 2013). Furthermore, analysis of the age ranges of the definite and probable clinical vCJD cases recorded in the UK reveals a striking age-related distribution

(Fig. S1). Of the 177 probable and definite cases reported to-date (August 2013), only 5 had occurred in eldery patients (2.8%; ≥60 years old), and 20 (11%) in middle aged individuals (~45-60 years old). Therefore, in order to study the effects of aging on prion pathogenesis in a laboratory mouse model, two age groups were used: young adult mice (six to eight weeks old), and immunosenescent aged (elderly) mice (~600 d old).

The splenic MZ is a specialized microenvironment which plays an important role in the capture and removal of blood-borne immune complexes, pathogens and their toxins (Mebius & Kraal, 2005). The continual shuttling of MZ B cells between the MZ and follicles is also important for the efficient delivery of blood-borne, complement-opsonized immune complexes to FDC (Cinamon *et al*., 2008). Prion replication upon PrP^{C}-expressing FDC is crucial for the efficient spread of infection to the CNS (Brown *et al*., 1999, Mabbott *et al*., 2000, McCulloch *et al*., 2013, Montrasio *et al*., 2000). Data suggest that an intact MZ is also required to facilitate the initial delivery of complement-opsonized prions to FDC (Brown *et al*., 2012). We have previously shown that the effects of aging on prion disease susceptibility are not simply due to reduced *Prnp* mRNA (which encodes PrP^{C}) expression levels in the CNS, or effects on the density or distribution of peripheral nerves in lymphoid tissues (Brown *et al*., 2012, Brown *et al*., 2009). Although aging-effects on other host factors cannot be entirely excluded, our data imply that the aging-related changes to FDC status and the MZ microarchitecture are likely to have had the major influence on prion disease susceptibility in the BSE-injected aged mice by impeding the initial delivery of prions into the B-cell follicles and reducing the availability of PrP^{C}-expressing

FDC. Similarly, the significant changes to the thickness and distribution of the $CD169^+$ MM macrophages in the MZ may also have impeded the delivery of prions to FDC in aged mice by aiding their sequestration and clearance.

In the aged spleens from each mouse strain there were highly significant reductions to the number and size of the PrP^C-expressing FDC networks, but small numbers of intact (PrP^C-expressing) FDC were evident. In the current study heavy PrP^d accumulations were detected upon the remaining intact FDC in the spleens of many of the BSE-challenged RIII mice, but in a much smaller proportion of spleens from aged C57BL mice. The reasons for these apparent mouse strain-specific differences in splenic PrP^d accumulation are uncertain. Both the RIII mice and C57BL mice share the same PrP genotype (*Prnp*^{a}; (Lloyd *et al*., 2004)). The effects of aging on the number and size of the PrP^c-expressing FDC networks were similar for each mouse strain, as was the aging-associated disruption to the network of MADCAM1-expressing sinus lining cells and the distribution and thickness of the $CD169^+$ MM macrophage layer in the MZ. However, the effects of aging in the distribution of $SIGNR1^+$ MZ macrophages differed between mouse strains: their distribution was significantly impaired in the MZ of aged C57BL mice, but appeared to be unaffected in aged RIII mice. C-type lectins such as SIGNR1 recognize specific carbohydrate structures that are present on cell-wall components of pathogens (Lanoue *et al*., 2004). Since the prion protein is highly glycosylated, it is plausible that SIGNR1 may play a similar role in the recognition and uptake of prions in the splenic MZ.

We have previously shown that whereas the susceptibility of aged mice to peripheral exposure with mouse-passaged scrapie prions was dramatically reduced, no effect on disease susceptibility was observed when prions were injected directly into the brain by intracerebral (i.c.) injection (Brown et al., 2012, Brown et al., 2009). However, in the current study aged mice were refractory to clinical prion disease after injection with primary BSE prions by combined i.c. and intraperitoneal injection. After peripheral exposure FDC are considered to amplify prions above the threshold required to achieve neuroinvasion (Mabbott, 2012, McCulloch et al., 2011). We have previously shown that young SCID mice which lack mature FDC in their spleens are also refractory to prion disease after i.c. injection with primary BSE prions (Brown et al., 1997). These data imply that the routing of prions through an intact lymphoreticular system is import for efficient neuroinvasion after cross-species transmission. These data also suggest that after interspecies prion exposure, the processing and replication of prions upon FDC in the peripheral lymphoid tissues is important for their adaptation to the new host and their ability to subsequently infect the nervous system. Data in the current study showing that the effects of aging on FDC status and the marginal zone are coincident with reduced prion disease susceptibility, are consistent with the reduced availability of replication sites (PrP^{C}-expressing FDC) in the spleen upon which the cattle BSE prions can adapt to the new host (mouse) environment, dramatically limiting their ability to replicate and subsequently spread to the brain.

Retrospective analyses prion-specific PrP^{Sc} accumulation in archived appendix and tonsil samples (Clewley *et al*., 2009, Hilton *et al*., 2002, Hilton *et al*., 2004)

suggest that the prevalence of vCJD in the UK population may be much higher than the clinical case data alone, implying the potential existence of a subclinical carrier state (Clewley *et al*., 2009, Garske & Ghani, 2010). Similarly, vCJD accumulation was detected in the spleen of an asymptomatic individual who was heterozygous (MV) at codon 129 of the prion protein gene (*PRNP* in humans) (Bishop *et al*., 2013, Peden *et al*., 2004). These data show that significant levels of vCJD prions can accumulate in the lymphoid tissues of infected individuals in the absence of observable clinical signs. These data suggest that the exposure of aged individuals to BSE may likewise have led to the accumulation of significant levels of vCJD prions within their lymphoid tissues in the absence of obvious clinical and histopathological signs of CNS involvement. Data presented here are consistent with data published elsewhere which show that low dose prion exposure (Thackray et al., 2003), immunodeficiency (Frigg et al., 1999) and cross-species prion transmission (Hill et al., 2000), like aging, can under some circumstances result in subclinical prion disease in affected individuals. However, in contrast to the above examples we did not observe significant evidence of PrP^{Sc} accumulation or neuropathology in the brains of any of the primary BSE-injected aged mice. Our data suggest that the effects of aging on FDC status and the MZ had impeded the replication of prions in the spleen, blocking or substantially delaying neuroinvasion.

Data in the current study raise important issues for human health and the potential for horizontal transmission of vCJD. We show that aged mice did not succumb to clinical prion disease during their life-spans after cross-species BSE exposure. However, many BSE-injected aged mice had detectable levels of PrP^{d}

in their spleens. Thus, although the combined effects of aging and the species barrier effect may represent a significant barrier to susceptibility to clinical disease after cross-species prion transmission, our data suggest there may be significant levels of prion accumulation in the lymphoid tissues of aged individuals in the absence of CNS involvement. The potential for the existence of a subclinical carrier state suggests a plausible risk for the horizontal spread of disease, for example after accidental iatrogenic exposure.

Materials and methods

Mice. C57BL/Dk and RIII mice were aged to ~600 d under specific-pathogen free conditions prior to use in subsequent studies. Young mice were six to eight weeks old at the time of analysis or use in subsequent studies. All experimental procedures were approved by the University of Edinburgh's ethical review process and conducted according to the strict regulations of the UK Home Office Animals (Scientific Procedures) Act 1986.

BSE agent exposure and disease monitoring. The BSE source used in this study was cattle brain homogenate from the brain of a clinically-affected UK Friesian Holstein cow (PG63/87) collected on 1/10/1987. This material has been used in a range of primary transmissions to mice at this Institute (eg: (Bruce et al., 1997, Fraser et al., 1992)) and produces a characteristic pattern in the mice consistent with classical BSE. Groups of C57BL and RIII (both of the *Prnp*^{a} genotype; (Lloyd *et al*., 2004)) were injected with a 10% (wt/vol) brain homogenate of cattle BSE by a combination of the i.c. (20 µl) and intraperitoneal (100 µl) routes (Brown *et al*., 1997, Bruce *et al*., 1997). These mouse strains were selected as previous transmissions of BSE show they produce highly reproducible incubation periods of disease and distinct patterns of vacuolar degeneration in their brains (Bruce *et al*., 1997). Following BSE exposure, mice were coded and assessed weekly for signs of clinical disease. The clinical endpoint of disease was determined by rating the severity of clinical signs of prion disease exhibited by the mice. Following clinical assessment, mice were scored as "unaffected", "possibly affected" and "definitely affected" using standard criteria which typically present in mice clinically-affected with prion

disease. The clinical endpoint of disease was defined in one of the following ways: i) the day on which a mouse received a second consecutive “definite” rating; ii) the day on which a mouse received a third “definite” rating within four consecutive weeks; iii) the day on which a mouse was culled in extremis.

The following criteria were used to help distinguish between the clinical signs of ageing (senility) in mice from those of prion disease (Brown *et al*., 2012). The fur of aged mice fur may lose colour and appear less sleek. Body shape may gradually change. Senile mice may have a “vacant stare” whereby the face looks thinner and the eyes not as bright. Mice beginning to display clinical signs of prion are often more motile and become more conspicuous, whereas those displaying definite positive signs are immobile and less interactive with their cage mates. In contrast, senile mice still move round their cages and interact with their cage mates. Survival times were recorded for mice that did not develop clinical signs of disease and were culled when they showed signs of intercurrent disease. Prion diagnosis was confirmed by histopathological assessment of vacuolation in the brain. For the construction of lesion profiles, vacuolar changes were scored in nine grey-matter areas of each brain as described (Bruce *et al*., 1997).

IHC. For the detection of disease-specific PrP (PrP^d) tissues were fixed 10% formal saline for 48 h and treated for 1h in 98% formic acid to reduce infectious BSE titre prior to *ex-vivo* analysis. Sections (thickness, 6 µm) were deparaffinised, and pre-treated to enhance the detection of PrP^d by hydrated autoclaving (15 min, 121 ºC, hydration) and subsequent immersion in formic acid

(98%) for 5 min (McBride *et al*., 1992). Sections were then immunostained with 1B3 PrP-specific polyclonal antiserum (Farquhar et al., 1989) or the PrP-specific monoclonal antibody (mAb) BH1 (Cancellotti et al., 2013). For the detection of astrocytes, brain sections were immunostained with anti-glial fibrillary acidic protein (GFAP; DAKO, Ely, UK). For the detection of microglia, deparaffinised brain sections were first pre-treated with Target Retrieval Solution (DAKO) and subsequently immunostained with anti-ionized calcium-binding adaptor molecule 1 (Iba-1; Wako Chemicals GmbH, Neuss, Germany). Immunolabelling was revealed using horseradish peroxidase conjugated to the avidin-biotin complex (HRP: Novared kit, Vector laboratories, Peterborough, UK). PET immunoblot analysis of brain was used to confirm that PrP^{d} detected by immunohistochemistry was PK-resistant PrP^{Sc}. Membranes were subsequently immunostained with 1B3 PrP-specific polyclonal antiserum and developed as described (Schulz-Schaeffer *et al*., 2000).

To compare the status of FDC and the MZ microarchitecture spleens were snap-frozen in liquid nitrogen and frozen sections (thickness, 10 µm) were fixed in acetone. FDC were visualised by staining with mAb FDC-M2 (212-MK-1FDCM2; ImmunoKontact) to detect complement component C4 and mAb 7G6 to detect CR2/CR1 (CD21/CD35; BD Pharmingen). Cellular PrP^{c} was detected using 1B3 PrP-specific polyclonal antiserum. The following rat-anti-mouse mAbs were used to define the MZ microarchitecture: mAb 2DD1 which recognizes the C-type lectin SIGNR1 expressed on MZ macrophages (eBioscience, San Diego, CA); mAb MOMA-1 (AbD Serotec, UK) which recognises CD169 expressed on MM macrophages; mAb MECA-367 which detects MAdCAM1 (AbD Serotec, UK) on the endothelial cells lining the MZ sinus. For immunofluorescent labelling

species-specific secondary antibodies coupled to Alexa Fluor 488 (green), Alexa Fluor 594 (red) or Alexa Fluor 647(blue) dyes (Invitrogen Life Technologies) were used. For visualisation at light level the avidin-biotin complex technique (HRP: Novared kit, Vector laboratories, Peterborough, UK) was used.

Semi-quantitative scoring of disturbances to MZ architecture. Well-oriented white pulp areas of spleen were selected at random from sections from four mice from each mouse group. MZ disruption was measured using a semi-quantitative scoring method (Fig. 5b-d & 6c) as described (Birjandi *et al*., 2011). Briefly, coded spleen sections were first immunostained to detect the marker of interest (CD169, MADCAM1, SIGNR1). The relative distortion of the splenic MZ was then characterized by comparing the following criteria: thickness of the cell layer; advancement cells of the MZ into the white pulp; presence of discontinuous ring of immunolabelling indicating disruption to the MZ. Grading of each image was scored as follows: 1, no disruption/minimal; 2, moderate; 3, severe (Fig. 5b & 5c). To quantify the MZ thickness, the depth of the cell layer was measured at three separate points from four randomly selected white pulp areas from four mice from each mouse group. For the quantitation of SIGNR1 expression on MZ macrophages, 4 randomly selected fields of view were collected from each mouse from each group and the % area of SIGNR1$^+$ immunolabeling in each field quantified using ImageJ software (http://rsbweb.nih.gov/ij/).

Image analysis and quantitation of PrP^c expression on FDC networks. The area of PrP^c expression upon FDC was quantified using ImageJ software as described previously (Brown *et al*., 2012, Brown *et al*., 2009, McCulloch *et al*.,

2011, McCulloch *et al*., 2013). From each spleen, three sections were studied and on each section data from three randomly selected fields of view containing individual FDC networks were collected. Therefore from each group data from a total of 36 individual FDC were analysed.

Statistical analyses. Data are presented as mean ± SE. Unless otherwise indicated, differences between groups were statistically compared using a student *t*-test. In instances where there was evidence of non-normality, data were analysed by a Mann-Whitney *U*-test. Values of $P < 0.05$ were accepted as significant.

Acknowledgements

This work was supported grant funding from the European Commission (FP7 project no. 222887: PRIORITY) and by Institute Strategic Programme Grant funding from the Biotechnology and Biological Sciences Research Council. The authors wish to thank Irene McConnell, Fraser Laing, Simon Cumming, Bob Fleming and the Pathology Services Group (The Roslin Institute & R(D)SVS, University of Edinburgh, UK) for excellent technical support; Christine Farquhar (The Roslin Institute & R(D)SVS) for provision of 1B3 anti-serum; Sandra McCutcheon for provision of mAb BH1 (The Roslin Institute & R(D)SVS); Prof. James Ironside (National CJD Research and Surveillance Unit, University of Edinburgh, UK) for data on the number of clinical vCJD cases in the UK, Rona Baron and Wilfred Goldmann for helpful discussion (The Roslin Institute & R(D)SVS).

References

Andreoletti, O., Berthon, P., Marc, D., Sarradin, P., Grosclaude, J., van Keulen, L., Schelcher, F., Elsen, J.-M. & Lantier, F. (2000). Early accumulation of PrP^{Sc} in gut-associated lymphoid and nervous tissues of susceptible sheep from a Romanov flock with natural scrapie. *J Gen Virol* **81**, 3115-3126.

Aydar, Y., Balogh, P., Tew, J. G. & Szakal, A. K. (2002). Age-related depression of FDC accessory functions and CD21 ligand-mediated repair of co-stimulation. *Eur J Immunol* **32**, 2817-2826.

Aydar, Y., Balogh, P., Tew, J. G. & Szakal, A. K. (2003). Altered regulation of FcgRII on aged follicular dendritic cells correlates with immunoreceptor tyrosin-based inhibition motif signaling in B cells and reduced germinal center formation. *J Immunol* **171**, 5975-5987.

Barron, R. M., Thomson, V., Jamieson, E., Melton, D. W., Ironside, J., Will, R. & Manson, J. C. (2001). Changing a single amino acid in the N-terminus of murine PrP alters TSE incubation time across three species barriers. *EMBO J* **20**, 5070-5078.

Birjandi, S. Z., Ippolito, J. A., Ramadorai, A. K. & Witte, P. L. (2011). Alterations in marginal zone macrophages and marginal zone B cells in old mice. *J Immunol* **186**, 3441-3451.

Bishop, M. T., Diack, A. B., Ritchie, D. L., Ironside, J. W., Will, R. G. & Manson, J. C. (2013). Prion infectivity in the spleen of a PRNP heterozygous individual with subclinical variat Creutzfedlt-Jakob disease. *Brain* **136**, 1139-1145.

Bishop, M. T., Hart, P., Aitchison, L., Baybutt, H. N., Plinston, C., Thomson, V., Tuzi, N. L., Head, M. W., Ironside, J. W., Will, R. G. & Manson, J. C. (2006). Predicting susceptibility and incubation time of human-to-human transmission of vCJD. *Lancet Neurol* **5**, 393-398.

Boelle, P.-Y., Cesbron, J.-Y. & Valleron, A.-J. (2004). Epidemiological evidence of higher susceptibility to vCJD in the young. *BMC Infect Dis* **4**, 7.

Bolton, D. C., McKinley, M. P. & Prusiner, S. B. (1982). Identification of a protein that purifies with the scrapie prion. *Science* **218**, 1309-1311.

Brown, K. L., Gossner, A., Mok, S. & Mabbott, N. A. (2012). The effects of host age on the transport of complement-bound complexes to the spleen and the pathogenesis of intravenous scrapie infection. *J Virol* **86**, 1228-1237.

Brown, K. L., Stewart, K., Bruce, M. E. & Fraser, H. (1997). Severly combined immunodeficient (SCID) mice resist infection with bovine spongiform encephalopathy. *J Gen Virol* **78**, 2707-2710.

Brown, K. L., Stewart, K., Ritchie, D., Mabbott, N. A., Williams, A., Fraser, H., Morrison, W. I. & Bruce, M. E. (1999). Scrapie replication in lymphoid tissues depends on PrP-expressing follicular dendritic cells. *Nat Med* **5**, 1308-1312.

Brown, K. L., Wathne, G. J., Sales, J., Bruce, M. E. & Mabbott, N. A. (2009). The effects of host age on follicular dendritic cell status dramatically impair scrapie agent neuroinvasion in aged mice. *J Immunol* **183**, 5199-5207.

Bruce, M. E., Will, R. G., Ironside, J. W., McConnell, I., Drummond, D., Suttie, A., McCardle, L., Chree, A., Hope, J., Birkett, C., Cousens, S., Fraser, H. & Bostock, C. J. (1997). Transmissions to mice indicate that 'new variant' CJD is caused by the BSE agent. *Nature* **389**, 498-501.

Cancellotti, E., Mahal, S. P., Somerville, R., Diack, A., Brown, D., Piccardo, P., Weissmann, C. & Manson, J. C. (2013). Post-translational changes to PrP alter transmissible spongiform encephalopathy strain properties. *EMBO J* **32**, 756-769.

Cinamon, G., Zachariah, M. A., Lam, O. M., Foss Jr, F. W. & Cyster, J. G. (2008). Follicular shuttling of marginal zone B cells facilitates antigen transport. *Nat Immunol* **9**, 54-62.

Clewley, J. P., Kelly, C. M., Andrews, N., K., V., Mallinson, G., Kaisar, M., Hilton, D. A., Ironside, J. W., Edwards, P., McCardle, L. M., D.L., R., Dabaghian, R., Ambrose, H. E. & Gill, O. N. (2009). Prevalence of disease related prion protein in anonymous tonsil specimens in Britain: cross sectional opportunistic survey. *Br Med J* **338**, b1442.

Farquhar, C. F., Somerville, R. A. & Ritchie, L. A. (1989). Post-mortem immunodiagnosis of scrapie and bovine spongiform encephalopathy. *J Virol Met* **24**, 215-222.

Fraser, H., Bruce, M. E., Chree, A., McConnell, I. & WElls, G. A. H. (1992). Transmission of bovine spongiform encephalopathy and scrapie to mice. *J Gen Virol* **73**, 1891-1897.

Frigg, R., Klein, M. A., Hegyi, I., Zinkernagel, R. M. & Aguzzi, A. (1999). Scrapie pathogenesis in subclinically infected B-cell-deficient mice. *J Virol* **73**, 9584-9588.

Garske, T. & Ghani, A. C. (2010). Uncertainty in the tail of the variant Creutzfeldt-Jakob disease epidemic in the UK. *PLoS ONE* **5**, e15626.

Ghani, A. C., Ferguson, N. M., Donnelly, C. A. & Anderson, R. M. (2000). Predicted vCJD mortality in Great Britain. *Nature* **406**, 583-584.

Hill, A. F., Joiner, S., Linehan, J., Desbrulais, M., Lantos, P. L. & Collinge, J. (2000). Species-barrier-independent prion replication in apparently resistant species. *Proc Natl Acadf Sci, USA* **97**, 10248-10253.

Hilton, D., Fathers, E., Edwards, P., Ironside, J. & Zajicek, J. (1998). Prion immunoreactivity in appendix before clinical onset of variant Creutzfeldt-Jakob disease. *Lancet* **352**, 703-704.

Hilton, D. A., Ghani, A. C., Conyers, L., Edwards, P., McCardle, L., Penney, M., Ritchie, D. & Ironside, J. W. (2002). Accumulation of prion protein in tonsil and appendix: review of tissue samples. *Br Med J* **325**, 633-634.

Hilton, D. A., Ghani, A. C., Conyers, L., Edwards, P., McCardle, L., Ritchie, D., Penney, M., Hegazy, D. & Ironside, J. W. (2004). Prevalence of lymphoreticular prion protein accumulation in UK tissue samples. *J Pathol* **203**, 733-739.

Houston, F., Goldmann, W., Chong, A., Jeffrey, M., Gonzalez, L., Foster, J., Parnham, D. & Hunter, N. (2003). Prion diseases: BSE in sheep bred for resistance to infection. *Nature* **423**, 498.

Klein, M. A., Kaeser, P. S., Schwarz, P., Weyd, H., Xenarios, I., Zinkernagel, R. M., Carroll, M. C., Verbeek, J. S., Botto, M., Walport, M. J., Molina, H., Kalinke, U., Acha-Orbea, H. & Aguzzi, A. (2001). Complement facilitates early prion pathogenesis. *Nat Med* **7**, 488-492.

Lanoue, A., Clatworthy, M. R., Smith, P., Green, S., Townsend, M. J., Jolin, H. E., Smith, K. G., Fallon, P. G. & McKenzie, A. N. (2004). SIGN-R1 contributes to protection against lethal pneumococcal infection in mice. *J Exp Med* **200**, 1383-1393.

Legname, G., Baskakov, I. V., Nguyen, H.-O. B., Riesner, D., Cohen, F. E., DeArmond, S. J. & Prusiner, S. B. (2004). Synthetic mammalian prions. *Science* **305**, 673-676.

Lloyd, S. E., Thompson, S. R., Beck, J. A., Lineham, J. M., Wadsworth, J. D. F., Brandner, S., Collinge, J. & Fischer, E. M. C. (2004). Identification and characterization of a novel prion gene allele. *Mammalian Genome* **15**, 383-389.

Mabbott, N. A. (2012). Prion pathogenesis and secodary lymphoid organs (SLO): Tracking the SLO spread of prions to the brain. *Prion* **6**, 322-333.

Mabbott, N. A., Bruce, M. E., Botto, M., Walport, M. J. & Pepys, M. B. (2001). Temporary depletion of complement component C3 or genetic deficiency of C1q significantly delays onset of scrapie. *Nat Med* **7**, 485-487.

Mabbott, N. A., Mackay, F., Minns, F. & Bruce, M. E. (2000). Temporary inactivation of follicular dendritic cells delays neuroinvasion of scrapie. *Nat Med* **6**, 719-720.

Mabbott, N. A., Young, J., McConnell, I. & Bruce, M. E. (2003). Follicular dendritic cell dedifferentiation by treatment with an inhibitor of the lymphotoxin pathway dramatically reduces scrapie susceptibility. *J Virol* **77**, 6845-6854.

McBride, P., Eikelenboom, P., Kraal, G., Fraser, H. & Bruce, M. E. (1992). PrP protein is associated with follicular dendritic cells of spleens and lymph nodes in uninfected and scrapie-infected mice. *J Pathol* **168**, 413-418.

McCulloch, L., Brown, K. L., Bradford, B. M., Hopkins, J., Bailey, M., Rajewsky, K., Manson, J. C. & Mabbott, N. A. (2011). Follicular dendritic cell-specific prion protein (PrP^{C}) expression alone is sufficient to sustain prion infection in the spleen. *PLoS Pathog* **7**, e1002402.

McCulloch, L., Brown, K. L. & Mabbott, N. A. (2013). Ablation of the cellular prion protein, PrP^{C}, specifcally on follicular dendritic cells has no effect on their maturation or function. *Immunology* **138**, 246-257.

Mebius, R. E. & Kraal, G. (2005). Structure and function of the spleen. *Nat Rev Immunol* **5**, 606-616.

Michel, B., Ferguson, A., Johnson, T., Bender, H., Meyerett-Reid, C., Pulford, B., von Teichman, A., Seelig, D., Weiss, J. H., Telling, G. C., Aguzzi, A. & Zabel, M. D. (2012). Genetic depletion of complement receptors CD21/35 prevents terminal prion disease in a mouse model of chronic wasting disease. *J Immunol* **189**, 4520-4527.

Montrasio, F., Frigg, R., Glatzel, M., Klein, M. A., Mackay, F., Aguzzi, A. & Weissmann, C. (2000). Impaired prion replication in spleens of mice lacking functional follicular dendritic cells. *Science* **288**, 1257-1259.

O'Connor, T., Frei, N., Sponarova, J., Schwarz, P., Heikenwalder, M. & Agguzi, A. (2012). Lymphotxin, but not TNF, is required for prion invasion of lymph nodes. *PLoS Pathog* **8**, e1002867.

Peden, A. H., Head, M. W., Ritchie, D. L., Bell, J. E. & Ironside, J. W. (2004). Preclinical vCJD after blood transfusion in a *PRNP* codon 129 heterozygous patient. *Lancet* **354**, 527-529.

Prusiner, S. B., Scott, M., Foster, D., Pan, K. M., Groth, D., Mirenda, C., Torchia, M., Yang, S. L., Serban, D., Carlson, G. A., Hoppe, P. C., Westaway, D. & DeArmond, S. J. (1990). Transgenic studies implicate interactions between homologous PrP isoforms in scrapie prion replication. *Cell* **63**, 673-686.

Schulz-Schaeffer, W. J., Tschoke, S., Kranefuss, N., Drose, W., Hause-Reitner, D., Giese, A., Groschup, M. H. & Kretzschmar, H. A. (2000). The paraffin-embedded tissue blot detects PrP^{sc} early in the incubation time in prion diseases. *Am J Pathol* **156**, 51-56.

Sigurdson, C. J., Williams, E. S., Miller, M. W., Spraker, T. R., O'Rourke, K. I. & Hoover, E. A. (1999). Oral transmission and early lymphoid tropism of chronic wasting disease PrP^{res} in mule deer fawns (*Odocoileus hemionus*). *J Gen Virol* **80**, 2757-2764.

Somerville, R. A., Hamilton, S. & Fernie, K. (2005). Transmissible spongiform encephalopathy strain, PrP genotype and brain region all affect the degree of glycosylation of PrP^{Sc}. *J Gen Virol* **86**, 241-246.

Taylor, P. R., Pickering, M. C., Kosco-Vilbois, M. H., Walport, M. J., Botto, M., Gordon, S. & Martinez-Pomares, L. (2002). The follicular dendritic cell restricted epitope, FDC-M2, is complement C4; localization of immune complexes in mouse tissues. *Eur J Immunol* **32**, 1883-1896.

Thackray, A. M., Klein, M. A. & Bujdoso, R. (2003). Subclinical prion disease induced by oral inoculation. *J Virol* **77**, 7991-7998.

Valleron, A.-J., Boelle, P.-Y., Will, R. & Cesbron, J.-Y. (2001). Estimation of epidemic size and incubation time based on age characteristics of vCJD in the United Kingdom. *Science* **294**, 1726-1728.

Wilesmith, J. W. (1993). BSE: Epidemiological approaches, trials and tribulations. *Preventative Vet Med* **18**, 33-42.

Will, R. G., Ironside, J. W., Zeidler, M., Cousens, S. N., Estibeiro, K., Alperovitch, A., Poser, S., Pocchiari, M. & Hofman, A. (1996). A new variant of Creutzfeldt-Jacob disease in the UK. *Lancet* **347**, 921-925.

Zabel, M. D., Heikenwalder, M., Prinz, M., Arrighi, I., Schwarz, P., Kranich, J., von Teichman, A., Haas, K. M., Zeller, N., Tedder, T. F., Weiss, J. H. & Aguzzi, A. (2007). Stromal complement receptor CD21/35 facilitates lymphoid prion colonization and pathogenesis. *J Immunol* **179**, 6144-6152.

Fig. 1. Effect of host age on the development of neuropathology (spongiform vacuolation) within the brain following primary BSE infection. (a & b) Histopathological analysis of brains BSE-injected young (closed circles) and aged (open circles) RIII (a) and C57BL mice (b). Vacuolation was scored on a scale of 1 to 5 in nine gray matter areas: 1, dorsal medulla; 2, cerebellar cortex; 3, superior colliculus; 4, hypothalamus; 5, thalamus; 6, hippocampus; 7, septum; 8, retrosplenial and adjacent motor cortex; 9, cingulate and adjacent motor cortex. Each point represents the mean vacuolation score ± SEM for groups of 9 to 14 mice. (c & d) Histopathological analysis of the spongiform vacuolation in the hypothalamus and cochlear nucleus of BSE-injected mice. Characteristic spongiform pathology were detected in the brains of clinically-affected RIII mice (c, upper panels) and C57BL mice (d, upper panels). However, no evidence of spongiform pathology was detected in any of the brains from the BSE-injected aged RIII mice (c, lower panels) and C57BL mice (d, lower panels). Representative images from the brains of control aged mice of equivalent ages are shown for comparison. Scale bar = 10 μm.

Fig. 2. Histopathological analysis of the characteristic signs of prion disease in the brains of the BSE-injected young and aged mice. (a) Cartoons illustrating the anatomical brain regions analysed. In young RIII mice (b) and C57BL mice (d) pathology consistent with terminal BSE infection was observed in the brains of all the clinically-affected mice. The typical neuropathological signs included heavy accumulations of disease specific PrP (PrP^d, brown, second column), reactive astrocytes expressing high levels of GFAP (brown, third column) and active microglia expressing Iba-1 (brown, fourth column). PET immunoblot analysis of

adjacent sections confirmed the PrP^d accumulations were PK-resistant PrP^{Sc} (black, first column). (c & e) In contrast, none of the aged mice had detectable histopathogical signs of prion disease in their brains. The exception was one clinically-negative, BSE-injected aged RIII mouse which had evidence of PrP^d accumulation only in the vestibular nucleus (see Fig. 3a).

Fig. 3. Comparison of the accumulation of disease-specific PrP (PrP^d) in the brains and spleens of BSE-injected young and aged mice. In contrast to the brains of clinically-affected young mice, the brains of all but one of the BSE-injected, clinically-negative aged RIII (a) and all of the BSE-injected, clinically-negative aged C57BL mice (b) lacked evidence of PrP^d accumulation (brown) in their brains. However, PrP^d accumulations were detected in the spleens of most (9/16) of the BSE challenged RIII mice (a) and 2/9 of the C57BL mice (b). Sections were counterstained with haematoxylin (blue). Arrow in "a" shows PrP^d accumulation in the vestibular nucleus. Scale bar = 20 µm.

Fig. 4. Effect of host age on FDC status in the spleen. Immunofluorescent analysis of FDC status in aged and young RIII mice (a) and C57BL mice (c). FDC in the spleens of young mice typically express high levels of the complement receptors CR2/CR1 (red) and cellular PrP^c (green) and trap complement component C4 (blue) on their surfaces of FDC (left-hand panels). In contrast, most of the FDC networks in the spleens of RIII mice and C57BL aged mice appeared to be disrupted and the expression of PrP^c and retention of complement component C4 and was dramatically reduced (right-hand panels). Scale bar = 50 µm. Morphometric analyses of the effect of host age on the size

of the CR2/CR1-expressing FDC networks, number and size of PrP^C-expressing FDC, and area of trapped C4 on the surface of FDC in the spleens of RIII mice (b) and C57BL mice (d). Differences between groups were analysed by a Mann-Whitney *U*-test.

Fig. 5. Effect of host age on the microarchitecture of the splenic MZ. (a) IHC analysis of the distribution of MADCAM1-expressing sinus lining cells (upper row, brown) and CD169-expressing MM macrophages (lower row, brown) in the MZ of young and aged RIII and C57BL mice. MZ, marginal zone; RP, red pulp; WP, white pulp; FO, FDC-containing B-cell follicle. Scale bar = 20 µm. (b) Semi-quantitative assessment of the effects of aging on the distribution to the layers of $MADCAM1^+$ sinus lining cells (b) and $CD169^+$ MM macrophages (c) in the spleen. Immunostained spleen sections were coded and four fields of view/mouse scored on a scale of 1 normal, to 3 severely disrupted. Representative images for each grade are shown. Differences between groups were analysed by a Student's *t*-test. (d) The effects of aging on the thickness of the layer of $CD169^+$ MM macrophages. Coded spleen sections from each mouse group were immunostained to detect CD169 (green) and the thickness of the cell layer measured at three distinct sites in four fields fields of view/mouse. Differences between groups were analysed by a Mann-Whitney *U*-test.

Fig. 6. Effect of host age on the distribution of C-type lectin SIGNR1-expressing MZ macrophages. (a & b) Comparison of SIGNR1 expression on MZ macrophages (red) and CD169 expression on MM macrophages (green) in the spleens of RIII mice (a) and C57BL mice (b). Typically, $CD169^+$ MM

macrophages are situated within an inner ring in the MZ whereas the SIGNR1$^+$ MZ macrophages are positioned within the outer border of the MZ. (a) In the spleens of aged RIII mice whereas the layer of CD169 MM macrophages was dramatically disrupted, the level of distribution of SIGNR1$^+$ MZ macrophages appeared similar to that observed in young mice. (b) In the spleens of aged C57BL mice the distribution of the CD169$^+$ MM macrophages and SIGNR1$^+$ MZ macrophages each appeared to be adversely affected when compared to young mice. MZ, marginal zone; RP, red pulp; WP, white pulp. Scale bar = 50 µm. (c) Morphometric analysis of the mean area of SIGNR1$^+$ pixels/image in spleens from each mouse group. Differences between groups were analysed by a Mann-Whitney *U*-test.

Supplementary Fig. 1. Number of variant Creutzfeldt-Jakob (vCJD) cases in the UK by 10 year age group. Data show the total number of definite (confirmed) and probable (without neuropathological confirmation) vCJD cases for each patient group up to August 2013. One probable/definite vCJD patient was alive at the time of analysis. These data were kindly supplied by Prof. James Ironside (National CJD Research & Surveillance Unit, University of Edinburgh, UK).

Fig. 1

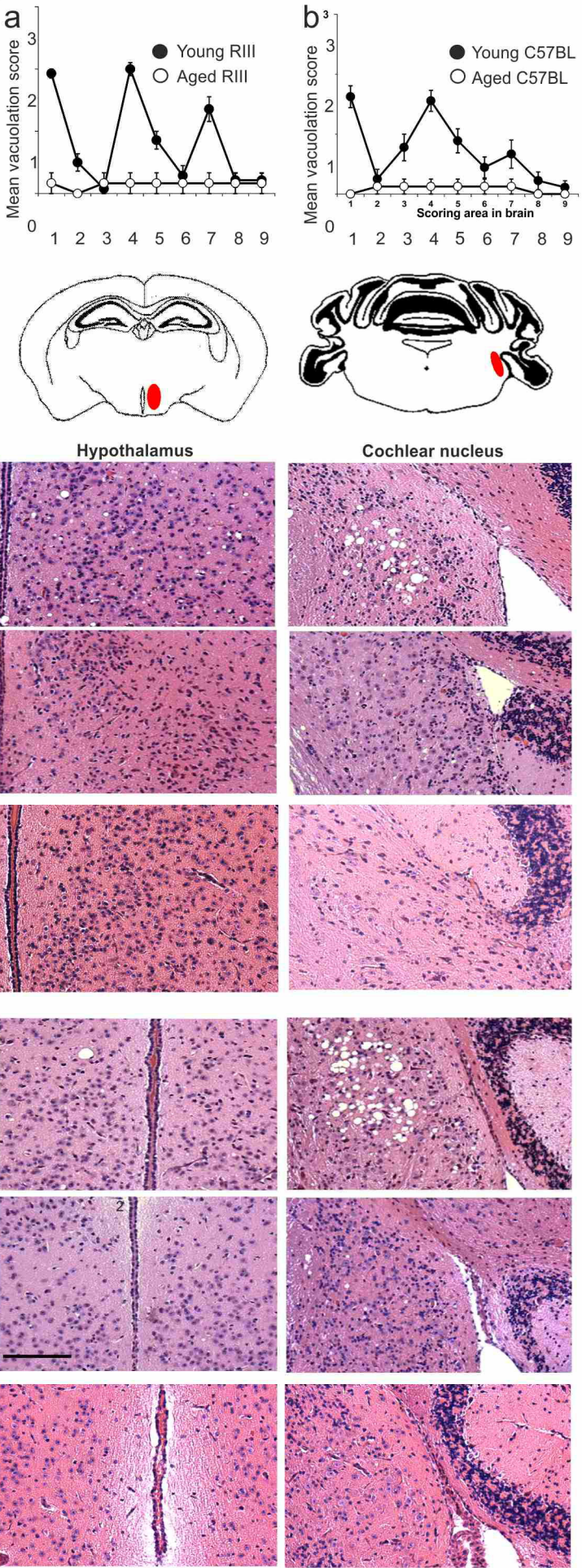
a
Mean vacuolation score
Young RIII
Aged RIII
b
Mean vacuolation score
Young C57BL
Aged C57BL
Scoring area in brain
c
Hypothalamus
Cochlear nucleus
RIII BSE-injected
Young
Aged
RIII control
Aged
d
C57BL BSE-injected
Young
Aged
C57BL control
Aged

Fig. 2

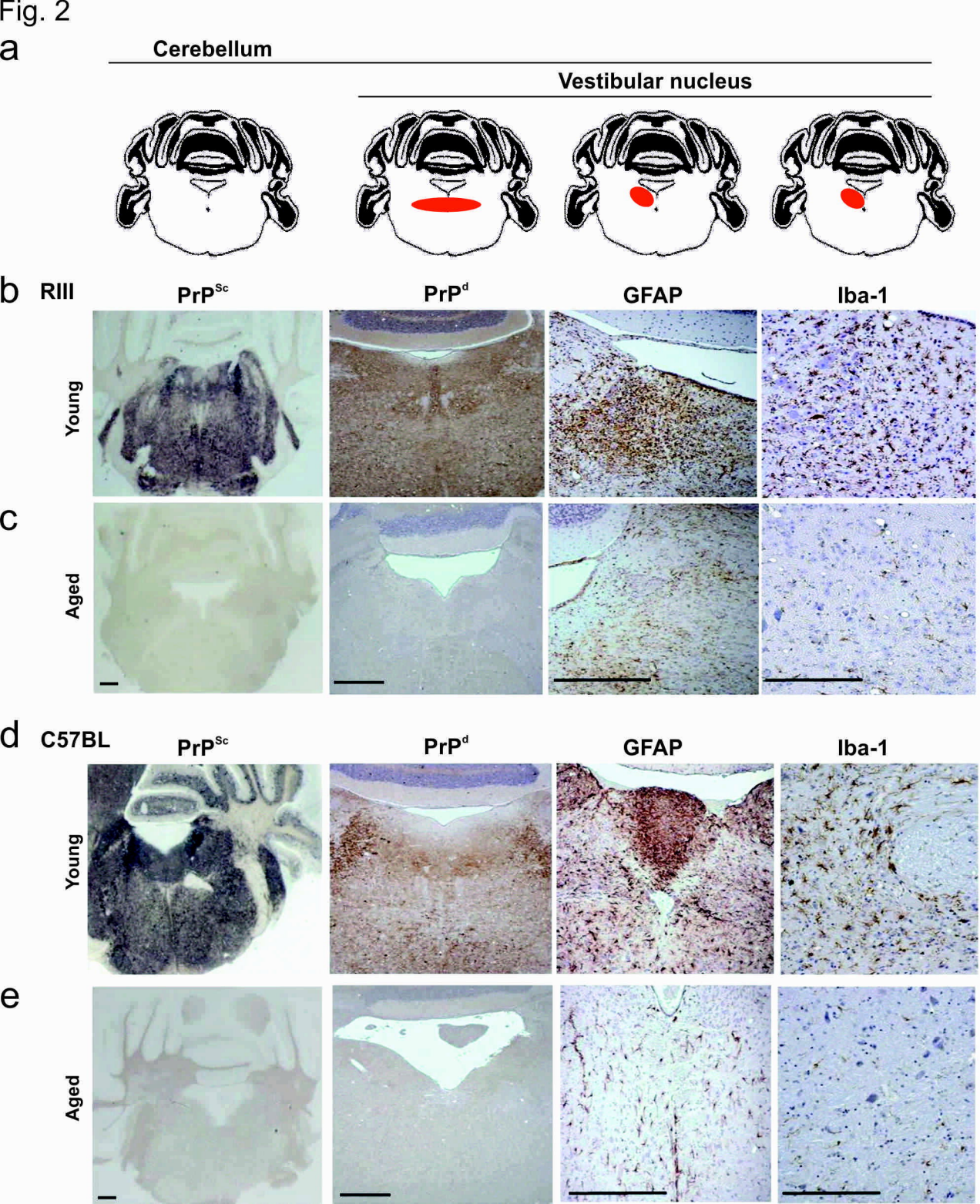
a
Cerebellum
Vestibular nucleus
b
RIII
PrP^Sc
PrP^d
GFAP
Iba-1
Young
c
Aged
d
C57BL
PrP^Sc
PrP^d
GFAP
Iba-1
Young
e
Aged

Fig. 3

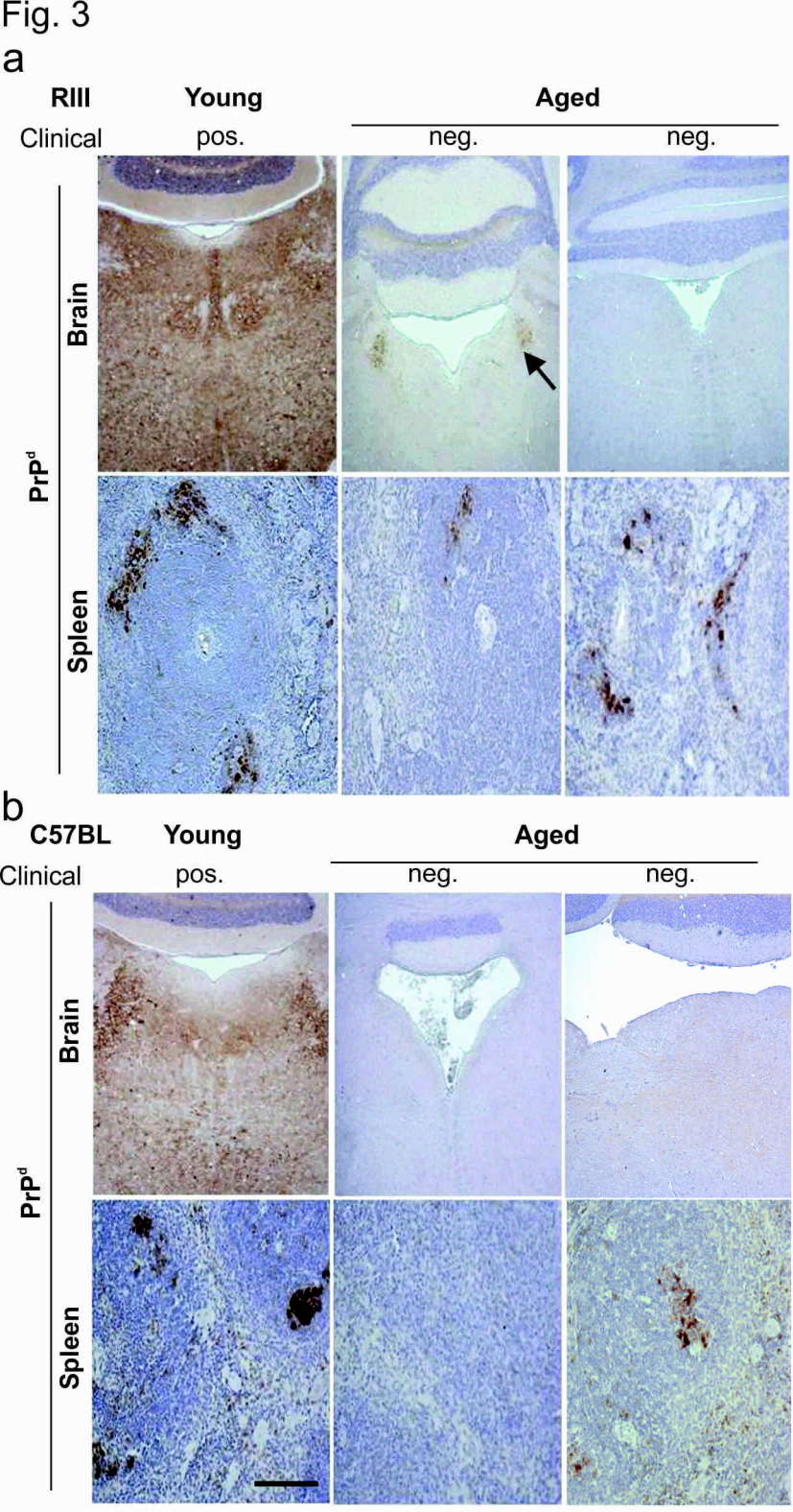
a
RIII
Young
Aged
Clinical
pos.
neg.
neg.
PrP^d
Brain
Spleen
b
C57BL
Young
Aged
Clinical
pos.
neg.
neg.
PrP^d
Brain
Spleen

Fig. 4

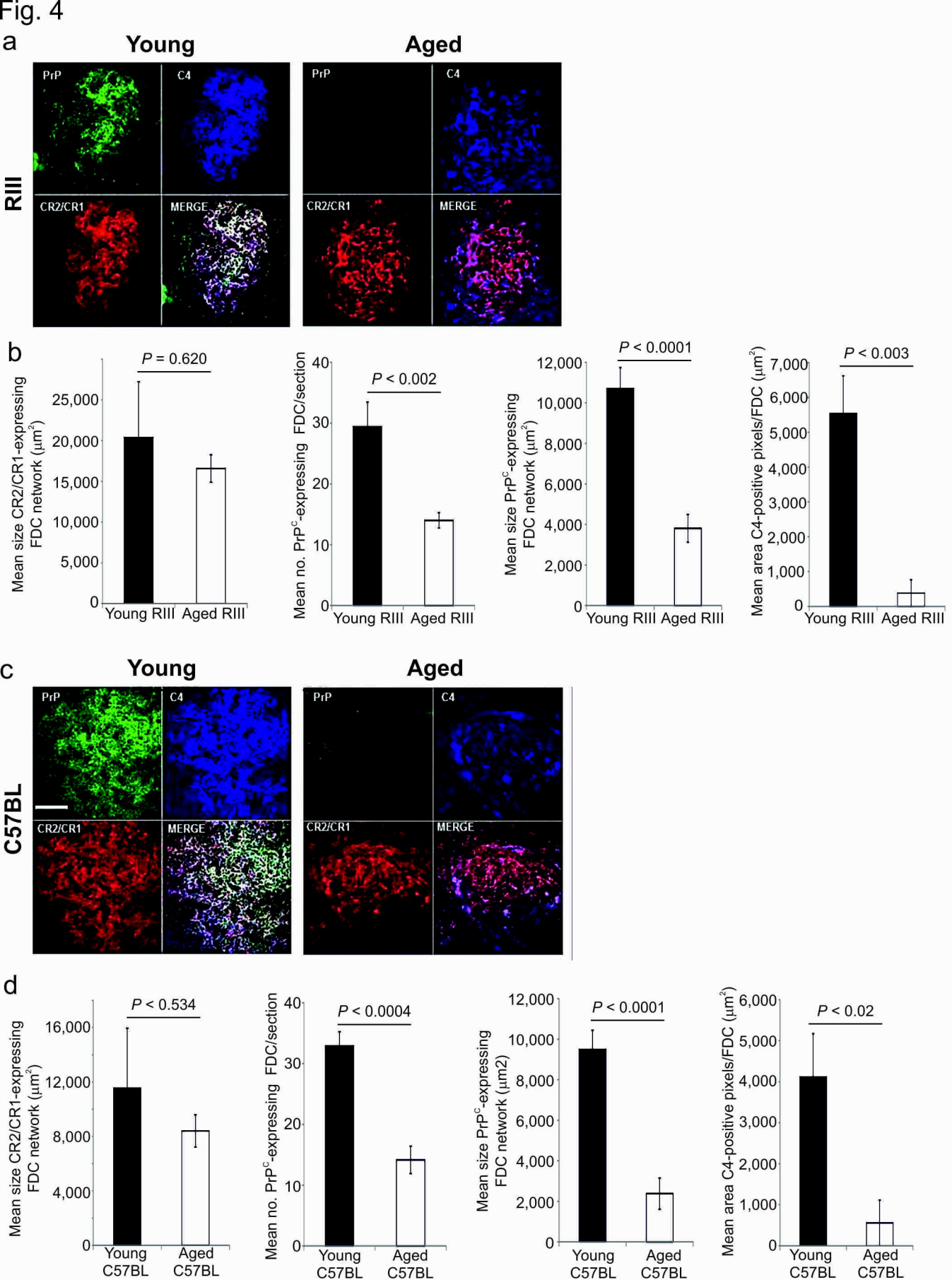
a
Young
Aged
RIII
PrP
C4
CR2/CR1
MERGE
b
P = 0.620
Mean size CR2/CR1-expressing FDC network (μm²)
25,000
20,000
15,000
10,000
5,000
0
Young RIII
Aged RIII
P < 0.002
Mean no. PrP^C-expressing FDC/section
40
30
20
10
0
P < 0.0001
Mean size PrP^C-expressing FDC network (μm²)
12,000
10,000
8,000
6,000
4,000
2,000
P < 0.003
Mean area C4-positive pixels/FDC (μm²)
7,000
6,000
5,000
4,000
3,000
2,000
1,000
c
C57BL
d
P < 0.534
Mean size CR2/CR1-expressing FDC network (μm²)
16,000
12,000
8,000
4,000
Young C57BL
Aged C57BL
P < 0.0004
Mean no. PrP^C-expressing FDC/section
P < 0.0001
Mean size PrP^C-expressing FDC network (μm2)
P < 0.02
Mean area C4-positive pixels/FDC (μm²)

Fig. 5

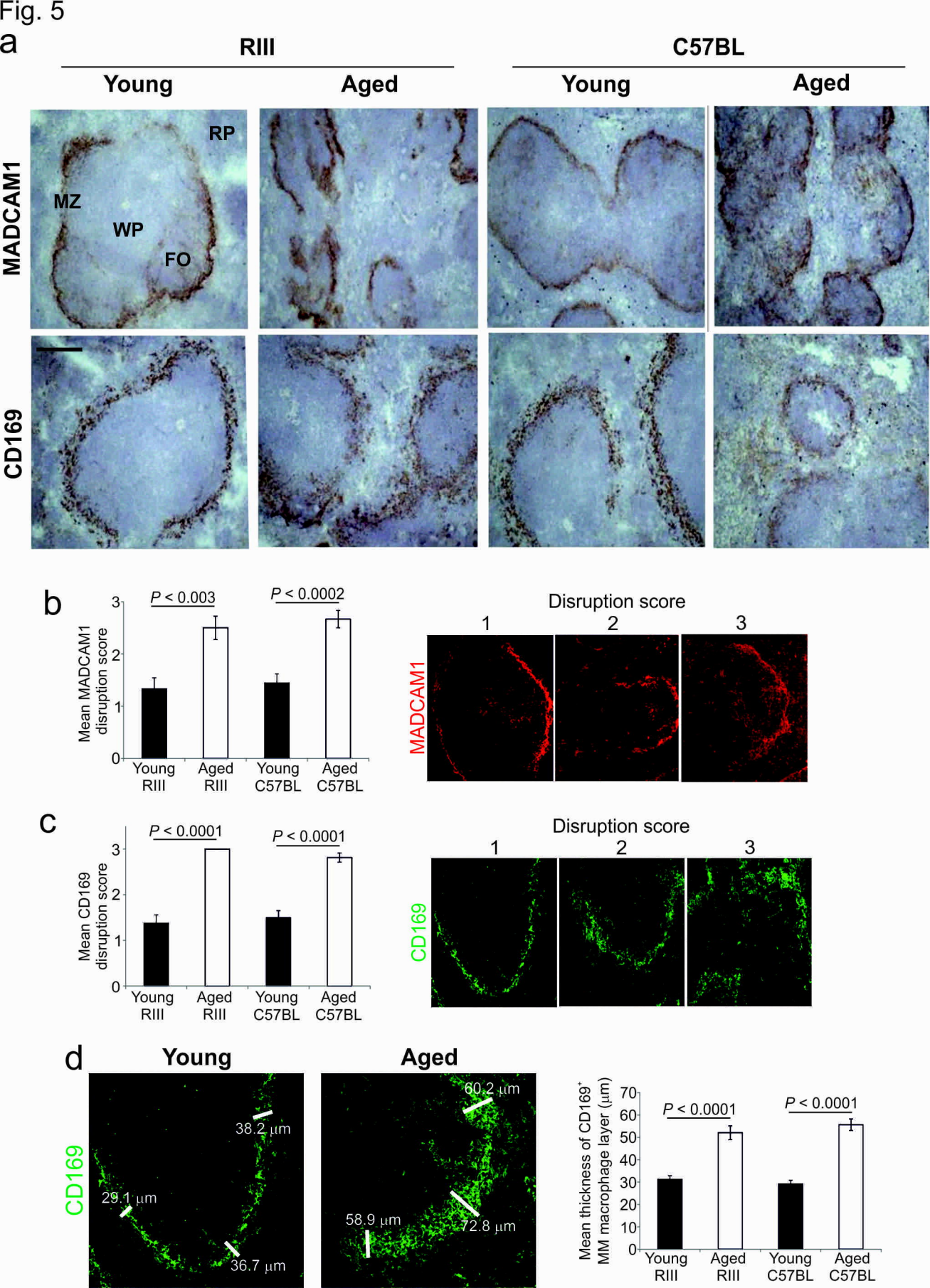
a
RIII
C57BL
Young
Aged
Young
Aged
MADCAM1
CD169
RP
MZ
WP
FO
b
P < 0.003
P < 0.0002
Mean MADCAM1 disruption score
Young RIII
Aged RIII
Young C57BL
Aged C57BL
Disruption score
1
2
3
MADCAM1
c
P < 0.0001
P < 0.0001
Mean CD169 disruption score
Young RIII
Aged RIII
Young C57BL
Aged C57BL
Disruption score
1
2
3
CD169
d
Young
Aged
CD169
38.2 μm
29.1 μm
36.7 μm
60.2 μm
58.9 μm
72.8 μm
P < 0.0001
P < 0.0001
Mean thickness of CD169+ MM macrophage layer (μm)
Young RIII
Aged RIII
Young C57BL
Aged C57BL

Fig. 6

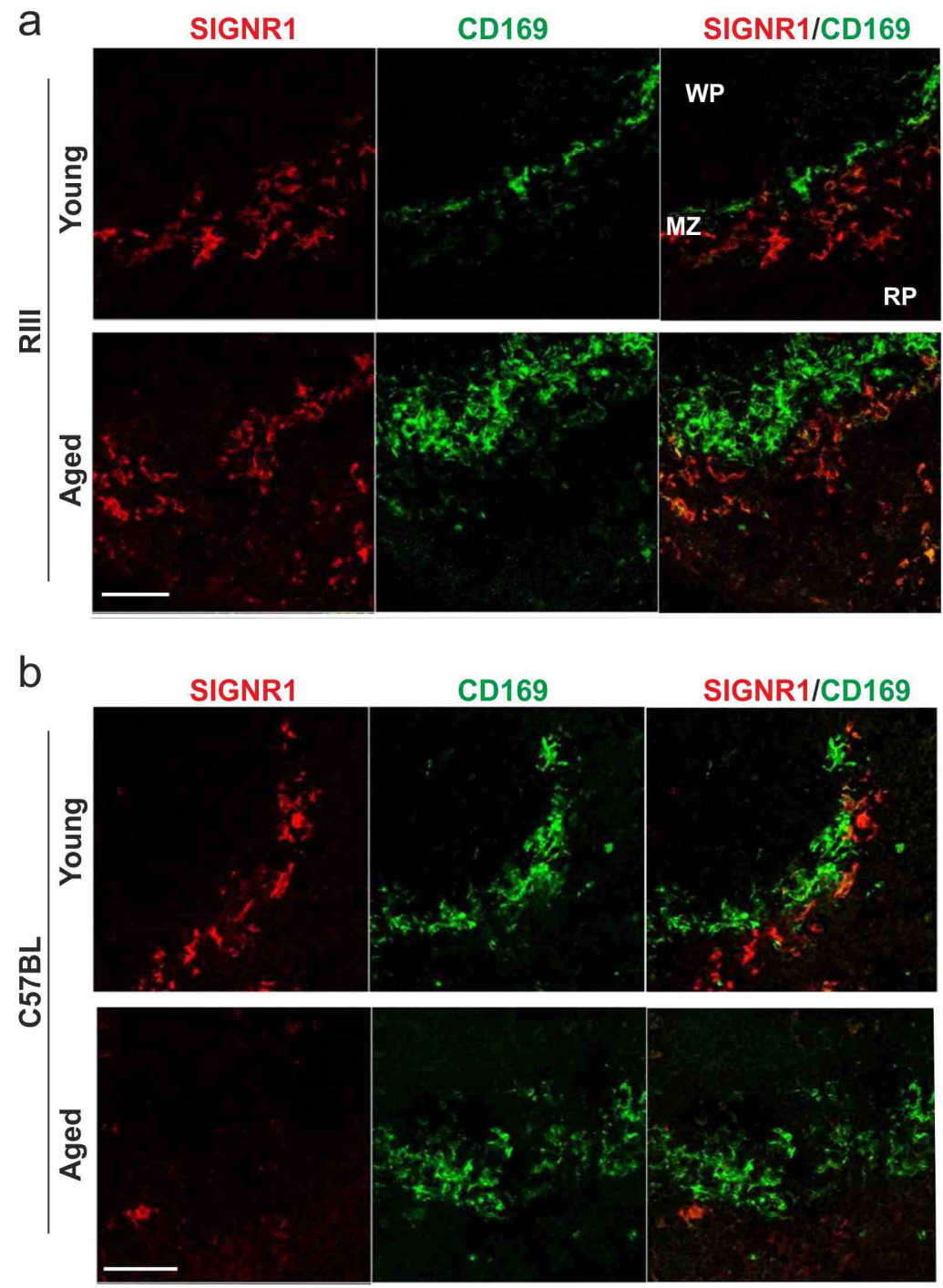
a
SIGNR1
CD169
SIGNR1/CD169
WP
MZ
RP
RIII
Young
Aged
b
SIGNR1
CD169
SIGNR1/CD169
C57BL
Young
Aged
c
Mean % area SIGNR1+ pixels
P = 0.16
P < 0.0003
0
1
2
3
Young RIII
Aged RIII
Young C57BL
Aged C57BL